

A Prototype Hand Geometry-based Verification System*

Anil K. Jain & Arun Ross
Michigan State University
East Lansing, MI 48824

Sharath Pankanti
IBM T.J. Watson Research Center
Yorktown Heights, NY 10598

Abstract

Geometric measurements of the human hand have been used for identity authentication in a number of commercial systems. Yet, there is not much open public literature addressing research issues underlying hand geometry-based identity authentication. This work is our attempt to draw attention to this important biometric by designing a prototype hand geometry-based identity authentication system. We also present our preliminary verification results based on hand measurements of 50 individuals captured over a period of time. The results are encouraging and we plan to address issues to improve the system performance.

1 Introduction

Associating an identity with an individual is called personal identification. The problem of resolving the identity of a person can be categorized into two fundamentally distinct types of problems with different inherent complexities: (i) verification and (ii) identification. Verification (authentication) refers to the problem of confirming or denying a person's claimed identity (Am I who I claim I am?). Identification (Who am I?) refers to the problem of establishing a subject's identity.

Biometrics involves identifying an individual based on his physiological or behavioral traits. The practical utility of biometrics-based identification is well established, as many systems require some sort of reliable user identification for servicing requests (e.g., ATM booths, cellular phones and laptop computers). Various biometric techniques have been described in the literature and many of them are being used for real-time authentication, the most popular ones being fingerprint identification and face recognition. Other biometrics that have resulted in commercial systems include iris scan, speech, retinal scan, facial thermograms and hand geometry.

In this paper we describe a verification system that uses the geometry of a person's hand to authenticate

his identity. A technique for computing the various features (invariant to the lighting conditions of the device, presence of noise and the color of the skin) is summarized. A prototype image acquisition system was developed to capture the profile of the hand. Our preliminary experiments on a database containing 50 users is presented.

2 Why Hand Geometry?

What is the most effective biometric measurement? There is no ideal biometric measurement; each biometric has its strengths and limitations, and accordingly each biometric appeals to a particular identification (authentication) application. Suitability of a particular biometric to a specific application depends upon several factors [8]; among these factors, the user acceptability seems to be the most significant. For many access control applications, like immigration, border control and dormitory meal plan access, very distinctive biometrics, e.g., fingerprint and iris, may not be acceptable for the sake of protecting an individual's privacy. In such situations, it is desirable that the given biometric indicator be only distinctive enough for verification but not for identification. As hand geometry information is not very distinctive, it is one of the biometrics of choice in applications like those mentioned above.

Hand geometry-based authentication is also very effective for various other reasons. Almost all of the working population have hands and exception processing for people with disabilities could be easily engineered [9]. Hand geometry measurements are easily collectible due to both the dexterity of the hand and due to a relatively simple method of sensing which does not impose undue requirements on the imaging optics. Note that good frictional skin is required by fingerprint imaging systems, and a special illumination setup is needed by iris or retina-based identification systems. Further, hand geometry is ideally suited for integration with other biometrics, in particular, fingerprints. For instance, an identification/verification system may use fingerprints for (infrequent) identification and use hand geometry for (frequent) verification.

*This work is partially supported by IBM Contract No. 444004069. Thanks to Dr. Mario Figueiredo for his assistance in formulating the parameter estimation problem.

It is easy to conceptualize a sensing system which can simultaneously capture both fingerprints and hand geometry.

3 Background

Hand Geometry, as the name suggests, refers to the geometric structure of the hand. This structure includes width of the fingers at various locations, width of the palm, thickness of the palm, length of the fingers, etc. Although these metrics do not vary significantly across the population, they can however be used to verify the identity of an individual. Hand geometry measurement is non-intrusive and the verification involves a simple processing of the resulting features. Unlike palmprint verification methods [7], this method does not involve extraction of detailed features of the hand (for example, wrinkles on the skin).

Hand geometry-based verification systems are not new and have been available since the early 1970s. However, there is not much open literature addressing the research issues underlying hand geometry-based identity authentication; much of the literature is in the form of patents [2, 3, 4] or application-oriented description. Sidlauskas [6] discusses a 3D hand profile identification apparatus that has been used for hand geometry recognition.

Authentication of identity of an individual based on a set of hand features is an important research problem. It is well known that the individual hand features themselves are not very descriptive; devising methods to combine these non-salient individual features to attain robust positive identification is a challenging pattern recognition problem in its own right. The research described here is our initial attempt to draw the attention of biometric researchers to this important yet neglected topic.

4 Image Acquisition

The image acquisition system which we have designed (inspired from [6, 9]) comprises of a light source, a camera, a single mirror and a flat surface (with five pegs on it). The user places his hand - palm facing downwards - on the flat surface of the device. The five pegs serve as control points for appropriate placement of the right hand of the user. The device also has knobs to change the intensity of the light source and the focal length of the camera. The lone mirror projects the side-view of the user's hand onto the camera. The device is hooked to a PC with a GUI application which provides a live visual feedback of the top-view and the side-view of the hand (Figure 1) and has the following functionality: (i) assists the user in correct positioning of the hand on the surface

of the device; (ii) acquires images of the user's hand; (iii) displays images that were captured previously; (iv) extracts features from a given image; (v) registers the user in a database along with the extracted feature vector; (vi) checks whether a given image of the hand matches any of the entries in the database; (vii) updates a particular user's entry in the database by recomputing the feature vector. In the current prototype implementation, a 640×480 8-bit grayscale image of the hand is captured.



Figure 1: Hand geometry sensing device.

4.1 Enrollment Phase

This process involves one of the following two tasks: (i) add a new user to the database; (ii) update a current user's feature vector. During the enrollment phase, five images of the same hand are taken in succession; the user removes his hand completely from the device before every acquisition. These five images are then used to compute the feature vector of the given hand. Recomputing a feature vector simply involves averaging the individual feature values.

4.2 Verification Phase

This process involves matching a given hand to a person previously enrolled in the system. Two snapshots of the hand are taken and the "average" feature vector is computed. The given feature vector is then compared with the feature vector stored in the database associated with the claimed identity. Let $F = (f_1, f_2, \dots, f_d)$ represent the d -dimensional feature vector in the database associated with the claimed identity and $Y = (y_1, y_2, \dots, y_d)$ be the feature vector of the hand whose identity has to be verified. The verification is positive if the distance between F and Y

is less than a threshold value. Four distance metrics, absolute, weighted absolute, Euclidean, and weighted Euclidean, corresponding to the following four equations were explored:

$$\sum_{j=1}^d |y_j - f_j| < \epsilon_a, \quad (1)$$

$$\sum_{j=1}^d \frac{|y_j - f_j|}{\sigma_j} < \epsilon_{wa}, \quad (2)$$

$$\sqrt{\sum_{j=1}^d (y_j - f_j)^2} < \epsilon_e, \text{ and} \quad (3)$$

$$\sqrt{\sum_{j=1}^d \frac{(y_j - f_j)^2}{\sigma_j^2}} < \epsilon_{we}, \quad (4)$$

where σ_j^2 is the feature variance of the j th feature and ϵ_a , ϵ_{wa} , ϵ_e , and ϵ_{we} are threshold values for each respective distance metric.

5 Feature Extraction

The hand geometry-based authentication system relies on geometric invariants of a human hand. Typical features include length and width of the fingers, aspect ratio of the palm or fingers, thickness of the hand, etc. [11]. To our knowledge, the existing commercial systems do not take advantage of any non-geometric attributes of the hand, e.g., color of the skin.

Figure 2 shows the 16 axes along which the various features mentioned above have been measured. The five pegs on the image serve as control points and assist in choosing these axes. The hand is represented as a vector of the measurements selected above. Since the positions of the five pegs are fixed in the image, no attempt is made to remove these pegs in the acquired images.

In order to offset the effects of background lighting, color of the skin, and noise, the following approach was devised to compute the various feature values. A sequence of pixels along a measurement axis will have an ideal gray scale profile as shown in Figure 3(a). Here Len refers to the total number of pixels considered, P_s and P_e refer to the end points within which the object (e.g., finger) to be measured is located, and $A1$, $A2$ and B are the gray scale values.

The actual gray scale profile tends to be spiky as shown in Figure 3(b). Our first step is to model the above profile. Let the pixels along a measurement axis be numbered from 1 to Len . Let $X = (x_1, x_2, \dots, x_{Len})$ be the gray values of the pixels along that axis. We make the following assumptions about the profile:

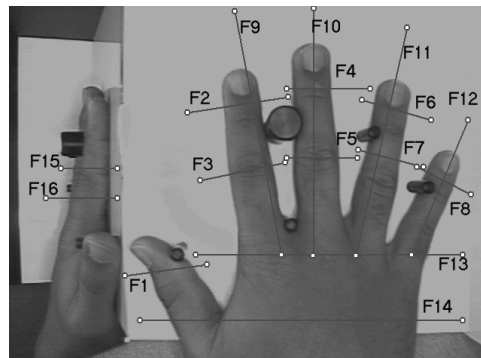


Figure 2: The sixteen axes along which feature values are computed.

1. The observed profile (Figure 3(b)) is obtained from the ideal profile (Figure 3(a)) by the addition of Gaussian noise to each of the pixels in the latter. Thus, for example, the gray level of a pixel lying between P_s and P_e is assumed to be drawn from the distribution

$$G(x/B, \sigma_B^2) = \frac{1}{\sqrt{2\pi\sigma_B^2}} \exp \left\{ -\frac{1}{2\sigma_B^2} (x - B)^2 \right\} \quad (5)$$

where σ_B^2 is the variance of x in the interval R , $P_s < R \leq P_e$.

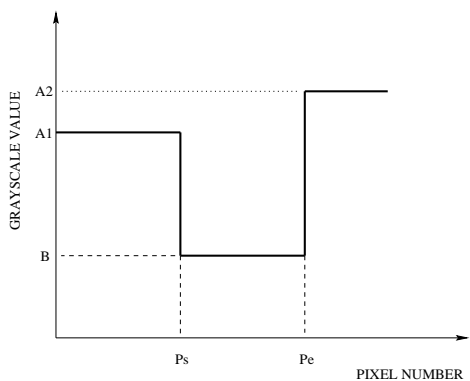
2. The gray level of an arbitrary pixel along a particular axis is *independent* of the gray level of other pixels in the line. This assumption holds good because of the absence of pronounced shadows in the acquired image.

Operating under these assumptions, we can write the joint distribution of all the pixel values along a particular axis as

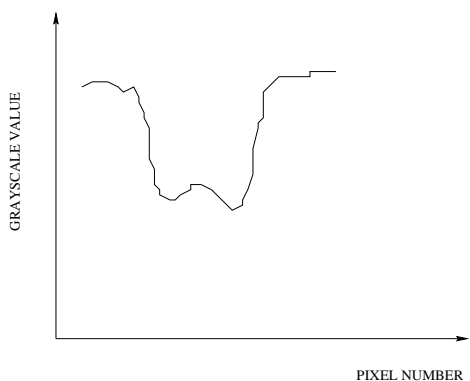
$$P(X/\Theta) = \left[\prod_{j=1}^{P_s} \frac{1}{\sqrt{2\pi\sigma_{A1}^2}} \exp \left\{ -\frac{1}{2\sigma_{A1}^2} (x_j - A1)^2 \right\} \right] \left[\prod_{j=P_s+1}^{P_e} \frac{1}{\sqrt{2\pi\sigma_B^2}} \exp \left\{ -\frac{1}{2\sigma_B^2} (x_j - B)^2 \right\} \right] \left[\prod_{j=P_e+1}^{Len} \frac{1}{\sqrt{2\pi\sigma_{A2}^2}} \exp \left\{ -\frac{1}{2\sigma_{A2}^2} (x_j - A2)^2 \right\} \right], \quad (6)$$

where $\Theta = (P_s, P_e, A1, A2, B, \sigma_{A1}^2, \sigma_{A2}^2, \sigma_B^2)$ and σ_{A1}^2 , σ_{A2}^2 and σ_B^2 are the variances of x in the three intervals $[1, P_s]$, $[P_s + 1, P_e]$ and $[P_e + 1, Len]$, respectively.

The goal now is to estimate P_s and P_e using the observed pixel values along the chosen axis. We use



(a) The ideal profile



(b) An observed profile

Figure 3: The gray scale profile of pixels along a measurement axis.

the Maximum Likelihood Estimate (MLE) method to estimate Θ . By taking logarithm on both sides of Eq. (6) and simplifying, we obtain the likelihood function:

$$\begin{aligned}
 L(\Theta) = & \frac{1}{\sigma_{A1}^2} \sum_1^{P_s} (x_j - A1)^2 + \frac{1}{\sigma_B^2} \sum_{P_s+1}^{P_e} (x_j - B)^2 \\
 & + \frac{1}{\sigma_{A2}^2} \sum_{P_e+1}^{Len} (x_j - A2)^2 + P_s \log \sigma_{A1}^2 \quad (7) \\
 & + (P_e - P_s) \log \sigma_B^2 + (Len - P_e) \log \sigma_{A2}^2
 \end{aligned}$$

The parameters can now be estimated iteratively; the parameter estimates at the $(k+1)^{st}$ stage, given the

observation $X = (x_1, x_2, \dots, x_{Len})$, are given below.

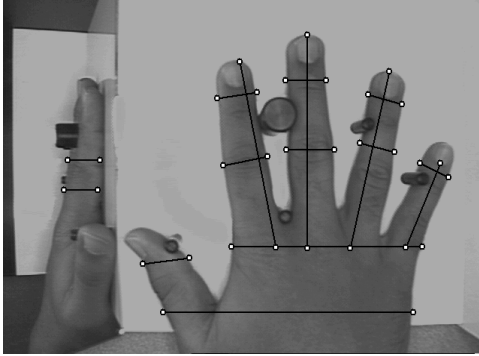
$$\begin{aligned}
 \widehat{P}_s^{(k+1)} &= \arg \min_{P_s} L \left(P_s, \widehat{P}_e^{(k)}, \widehat{A1}^{(k)}, \widehat{A2}^{(k)}, \right. \\
 & \quad \left. \widehat{B}^{(k)}, \widehat{\sigma}_{A1}^2^{(k)}, \widehat{\sigma}_{A2}^2^{(k)}, \widehat{\sigma}_B^2^{(k)} \right) \\
 \widehat{P}_e^{(k+1)} &= \arg \min_{P_e} L \left(\widehat{P}_s^{(k+1)}, P_e, \widehat{A1}^{(k)}, \widehat{A2}^{(k)}, \right. \\
 & \quad \left. \widehat{B}^{(k)}, \widehat{\sigma}_{A1}^2^{(k)}, \widehat{\sigma}_{A2}^2^{(k)}, \widehat{\sigma}_B^2^{(k)} \right) \\
 \widehat{B}^{(k+1)} &= \frac{\sum_{\widehat{P}_s^{(k+1)}+1}^{\widehat{P}_e^{(k+1)}} x_j}{\widehat{P}_e^{(k+1)} - \widehat{P}_s^{(k+1)}} \\
 \widehat{\sigma}_B^2^{(k+1)} &= \frac{\sum_{\widehat{P}_s^{(k+1)}+1}^{\widehat{P}_e^{(k+1)}} x_j^2}{\widehat{P}_e^{(k+1)} - \widehat{P}_s^{(k+1)}} - \left\{ \widehat{B}^{(k+1)} \right\}^2 \\
 \widehat{A1}^{(k+1)} &= \frac{\sum_1^{\widehat{P}_e^{(k+1)}} x_j}{\widehat{P}_s^{(k+1)}} \\
 \widehat{\sigma}_{A1}^2^{(k+1)} &= \frac{\sum_1^{\widehat{P}_e^{(k+1)}} x_j^2}{\widehat{P}_s^{(k+1)}} - \left\{ \widehat{A1}^{(k+1)} \right\}^2 \\
 \widehat{A2}^{(k+1)} &= \frac{\sum_{\widehat{P}_e^{(k+1)}+1}^{Len} x_j}{Len - \widehat{P}_e^{(k+1)}} \\
 \widehat{\sigma}_{A2}^2^{(k+1)} &= \frac{\sum_{\widehat{P}_e^{(k+1)}+1}^{Len} x_j^2}{Len - \widehat{P}_e^{(k+1)}} - \left\{ \widehat{A2}^{(k+1)} \right\}^2 \quad (8)
 \end{aligned}$$

The initial estimates of $A1$, σ_{A1}^2 , $A2$, σ_{A2}^2 , B and σ_B^2 are obtained as follows: (i) $A1$ and σ_{A1}^2 are estimated using the gray values of the first N_{A1} pixels along the axis; (ii) $A2$ and σ_{A2}^2 are estimated using the gray values of the pixels from $(Len - N_{A2})$ to Len ; (iii) B and σ_B^2 are estimated using the gray values of the pixels between $(Len/2 - N_B)$ and $(Len/2 + N_B)$. The values of N_{A1} , N_{A2} and N_B are fixed for the system; $N_{A1} = 5$, $N_{A2} = 4$ and $N_B = 5$. The initial values of P_s and P_e are set to $Len/2 - 10$ and $Len/2 + 10$, respectively.

Figure 4 shows a hand image along with the positions of detected points (P_s and P_e) along each of the 16 axes and the corresponding feature vector.

6 Experimental Results

The hand geometry authentication system was trained and tested using a database of 50 users. Ten images of each user's hand were captured over two sessions; in each session the background lighting of the acquisition device was changed. Thus a total of 500 images were made available. Out of 500 images, only 360 were used for testing our hand geometry system. The remaining 140 images were discarded due to



(a) Estimates of P_s and P_e along the 16 axes

(akasapuv 65 53 59 52 62 47 47 45 255 333 253 287 243 149 34 35)

(b) The corresponding database entry

Figure 4: Computation of the feature vector.

incorrect placement of the hand by the user (see for example, Figure 6). Thus, user adaptation of this biometric is necessary. Two images of each user's hand were randomly selected to compute the feature vector which is stored in the database along with the user's name. Figure 5 shows the Chernoff faces [12] representing the average feature vector of 20 of the users. 15 hand features have been mapped to the attributes of the cartoon face as follows: 1-area of face; 2-shape of face; 3-length of nose; 4-location of mouth; 5-curve of smile; 6-width of mouth; 7, 8, 9, 10 and 11-location, separation, angle, shape and width of eyes; 12-location and width of pupil; 13, 14 and 15 -location, angle and width of eyebrow. The difference between any two hand geometries as reflected in these cartoon faces appears to be significant.

Eqs. (1)-(4) are used for verifying whether the feature vector of a hand matches with the feature vector stored in the database. In order to study the effectiveness of various distance metrics, the genuine and impostor distributions are plotted for matching scores obtained using each distance metric and a ROC generated from each pair of distributions. A genuine matching score is obtained by comparing two feature vectors from the same hand while an impostor matching score is obtained by comparing the feature vectors of two different hands. Let us define the hit rate to be the percentage of time the system matches a hand to the right entry in the database, and the false accep-

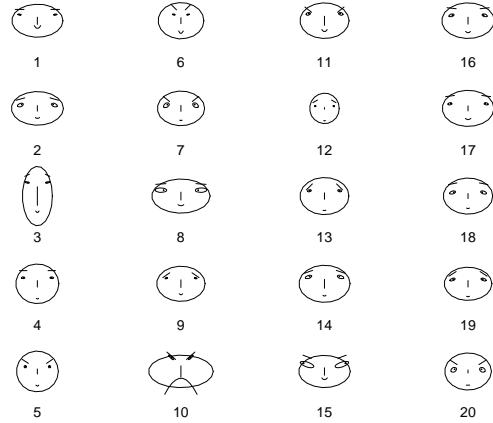


Figure 5: Chernoff Faces representing the average feature vectors of 20 different hands.



Figure 6: Incorrect placement of hand.

tance rate to be the percentage of time the system matches a hand to an incorrect entry in the database for a given threshold. The ROC that plots the hit rate against the false acceptance rate is then computed using the leave-one-out method. A feature vector in the database is matched against those feature vectors representing a different user. The minimum of these distances is taken as an impostor matching score. If the matching score falls below the chosen threshold, it is considered to be a false acceptance by the system. This process is repeated for all the users in the database. A genuine matching score is obtained by matching a feature vector against those feature vectors that belong to the same user and then taking the minimum of all such distances. If the matching score falls below the chosen threshold then it is considered

to be a hit. The ROC shown in Figure 7 depicts the performance of the system for the weighted Euclidean distance (Eq. 4) which gave the best result. The system performance could be significantly improved by (i) having habituated users; (ii) better registration of hand geometry measurements; and (iii) using higher level features (like color of the skin, wrinkles and folds on the skin etc.). Among these factors, registration appears to be the most critical. Even though the pegs are used for registration in our system, the registration accomplished by the pegs is not sufficiently accurate.

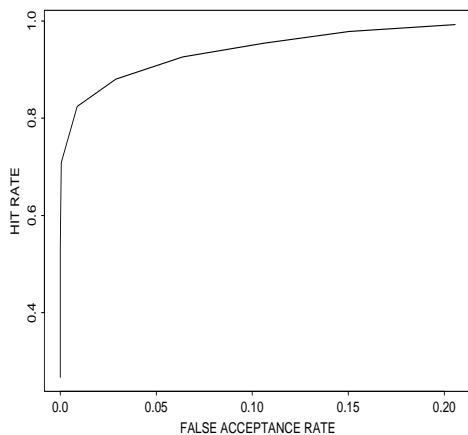


Figure 7: Receiver Operating Curve

7 Future Work

We have designed a prototype hand geometry-based verification system and presented our initial identity authentication results based on the hand-geometry measurements of 50 individuals. We have presented an end-to-end technological description of the design/implementation/evaluation of the hand geometry based authentication. Our ongoing work is investigating imaging set up, feature extraction, and a theoretical framework for matching. In particular, we are concentrating on the following problems: (i) The present imaging involves visible light. It would be interesting to explore the effects of infra-red imaging on the system performance. We also plan to investigate the effects of different resolutions and color planes on the system performance. (ii) The existing feature set should be extended to include 2-D features of the hand. We plan to use deformable models for a robust representation of the hand. (iii) A more extensive system performance on larger datasets collected over a period of time is necessary. (iv) Integration of hand geometry information with other biometrics,

e.g., fingerprints, would require designing a new image acquisition setup. With the availability of solid-state fingerprint sensors [13], this is now feasible.

References

- [1] A.K. Jain, R. Bolle and S. Pankanti (Eds.), "Biometrics: Personal Identification in Networked Society", *Kluwer Academic Publishers*, 1998.
- [2] R. P. Miller, "Finger dimension comparison identification system", *US Patent No. 3576538*, 1971.
- [3] R. H. Ernst, "Hand ID system", *US Patent No. 3576537*, 1971.
- [4] I. H. Jacoby, A. J. Giordano, and W. H. Fioretti, "Personnel Identification Apparatus", *US Patent No. 3648240*, 1972.
- [5] "A Performance Evaluation of Biometric Identification Devices", *Technical Report SAND91-0276, UC-906, Sandia National Laboratories, Albuquerque, NM and Livermore, CA*, 1991.
- [6] D. P. Sidlauskas, "3D hand profile identification apparatus", *US Patent No. 4736203*, 1988.
- [7] J. R. Young and H. W. Hammon, "Automatic Palmprint Verification Study", *Rome Air Development Center, RADC-TR-81-161 Final Technical Report*, June 1981.
- [8] A. Jain, L. Hong, S. Pankanti, and R. Bolle, "Online identity-authentication system using fingerprints," *Proceedings of IEEE*, vol. 85, pp. 1365–1388, September 1997.
- [9] R. Zunkel, "Hand Geometry Based Authentication" in "Biometrics: Personal Identification in Networked Society", A. Jain, R. Bolle, and S. Pankanti (Eds.), *Kluwer Academic Publishers*, 1998.
- [10] "INS Passenger Accelerated Service System (INSPASS)," <http://www.biometrics.org:8080/~BC/REPORTS/INSPASS.html>, 1996.
- [11] "HaSIS - A Hand Shape Identification System", <http://www.csr.unibo.it/research/biolab/hand.htm>.
- [12] Chernoff, H., "The use of Faces to Represent Points in k-Dimensional Space Graphically", *Journal of the American Statistical Association*, 68, 361-368, 1973.
- [13] "Veridicom Fingerprint Sensor for OEMS", <http://www.veridicom.com/fps100frames.htm>.